TITLE

Diversification of perceptual mechanisms underlying preserved multisensory behavior in healthy aging

AUTHORS/AFFILIATIONS

Hame Park[1,2], Julia Nannt[1,2], Christoph Kayser[1,2]

[1]Department for Cognitive Neuroscience, Faculty of Biology, Bielefeld University, Universitätsstr. 25, 33615, Bielefeld, Germany.

[2]Center for Cognitive Interaction Technology (CITEC), Bielefeld University, Inspiration 1, 33615, Bielefeld, Germany.

ABSTRACT

The perceptual use of multisensory information apparently changes with age. Yet it remains unclear whether previously reported age-effects arise from changes in the sensory computations by which information is combined, from a reduced sensory precision with age, or changes in the belief that different sensory-motor cues are causally linked. To address this question we analysed how healthy young and older adults integrate audio-visual information within (ventriloquist-effect) and between trials (ventriloquist after-effect) using models of Bayesian causal inference. Despite a reduced precision of sensory representations in the elderly, both groups exhibited comparable ventriloquist biases that were reproduced by largely the same sensory computations. While the after-effect bias was also comparable between groups, modelling showed that this was driven by previous sensory information in younger but by the previous response in older participants. This suggests a transition from a sensory- to a behavior-driven influence of past experience on subsequent choices with age, possibly related to the reduced sensory precision or memory capacity with age.

KEYWORDS

Aging, multisensory integration, multisensory recalibration, Ventriloquist effect, Ventriloquist after-effect, Bayesian causal inference

1. INTRODUCTION

One of the commonly known features of healthy aging is losing the 'sharpness' - such as the precision of sensory perception (Dobreva et al., 2011; Lindenberger and Baltes, 1994; Otte et al., 2013; Salthouse, 1996), that of memory (Salthouse, 2019, 2010), or the swiftness of responses (Falkenstein et al., 2006; Jones et al., 2019). Such changes in perception are accompanied by alterations in brain structure or brain activity with age (Henry et al., 2017; Henschke et al., 2018; McNair et al., 2019), suggesting that aging may affect both early sensory and higher level cognitive processes (Diaconescu et al., 2013; Dully et al., 2018; Henry et al., 2017; McNair et al., 2019; Nunez, 2015; Zanto and Gazzaley, 2014). Unravelling the mechanisms by which perception changes with age becomes particularly challenging when behavior relies on the combination of multiple sensory or behavioral attributes, such as during multisensory integration or the adaptive trial-by-trial recalibration of perception based on previous experience (also known as after-effects). Here, age-related changes in behavior performance could result from a number of sources, ranging from a decline in the precision of the individual sensory representations to changes in the decision rules or the computational principles by which different features are combined (Jones et al., 2019).

Previous studies have described a number of ways in which multisensory perception seems to change with age (Freiherr et al., 2013): older adults seem to benefit more from multisensory information during speeded detections (Diaconescu et al., 2013), older adults are more strongly influenced by task-irrelevant distractors (Dobreva et al., 2012), have wider temporal binding windows (Bedard and Barnett-Cowan, 2016; Chan et al., 2014a; Diederich et al., 2008), and sacrifice response speed to preserve accuracy (Jones et al., 2019). Furthermore, the persistent influence of previous information on subsequent decisions changes with age. For example, the adaptation to audio-visual synchrony and the recalibration during temporal binding are both attenuated in older adults (Bedard and Barnett-Cowan, 2016; Chan et al., 2014b; Noel et al., 2016; Vercillo et al., 2017). Despite these widespread changes in multisensory perception with age, the underlying mechanisms remain debated. While some studies

suggested that a reduced precision of sensory representations is the key drive of these changes (Dobreva et al., 2012; Lindenberger and Baltes, 1994; Trelle et al., 2019; Tye-Murray et al., 2016), others speculated whether the nature of the multisensory sensory computations themselves may change (Baum and Stevenson, 2017; Diederich et al., 2008; Mozolic et al., 2012).

The focus of this study was to understand the nature of potential age-related changes in audio-visual spatial perception. We compared changes in two multisensory response biases between young (18 ~ 35 years) and older (62 ~ 82 years) healthy participants: the within-trial integration of multisensory information (the ventriloquist effect) and the trial-by-trial recalibration of unisensory perception based on a previous multisensory stimulus (the so-called ventriloquist after-effect). Using the framework of Bayesian causal inference (Angelaki et al., 2009; Jones et al., 2019; Körding et al., 2007; Rohe and Noppeney, 2015a; Wozny et al., 2010) we compared four candidate factors that could explain differences in multisensory behavior between groups: first, the precision of unisensory representations; second, the a priori belief that sequential experiences are causally linked and hence should be combined for a subsequent behavior; third, the decision rules used to forge sensory estimates derived from different causal models underlying the received multisensory information; and fourth, the ability of the same computational architectures to account for the behavioral data of younger and older participants. In brief, our results show that both multisensory integration and recalibration are preserved with age, despite a decline of sensory precision with age. However, they also show that the mechanism by which previous experience shapes subsequent behavior during trial-by-trial recalibration changes with age, shifting from a sensory-driven to a behavior-driven influence of past experience on subsequent choices.

2. METHODS

2.1. Participants

24 healthy right-handed younger adults (YA, 9 males, mean age 23.5 years, range 18 ~ 35 years) and 24 healthy right-handed older adults (OA, 7 males, mean age 69.0 years, range 62 ~ 82 years) participated in this study. The sample size was determined based on previous studies using similar experimental protocols (Jones et al., 2019) and recommendations for sample sizes in empirical psychology (Simmons et al., 2011). All participants submitted informed written consent. The YA had self-reported normal vision and hearing and indicated no history of neurological diseases. OA's were

screened for normal vision and hearing: pure-tone audiometric thresholds were obtained at 500 Hz, 1000 Hz, and 2000 Hz and individuals with average thresholds higher than 30 dB for either ear were excluded (mean ± SD thresholds for included participants: 14.1 dB ± 6.4 dB, 13.8 dB ± 6.8 dB for the left and right ear respectively). The visual acuity was 20/25 or 20/20 for all OA participants. OA were also tested on the Montreal Cognitive Assessment (MoCA) (Nasreddine et al., 2005) and all OA's scored above 26, indicating no cognitive impairment (mean ± SD: 28.8 ± 1.56). Data from two YA (both females) had to be excluded as they were not able to perform the task correctly. One OA did not pass the hearing test and two did not pass the spatial hearing test (see below; both females). Therefore, data are reported for a sample of 22 YA and 21 OA.

2.2. *Stimuli*

The acoustic stimulus was a 1300 Hz sine wave tone (50 ms duration) sampled at 48 kHz and presented at 64 dB r.m.s. through one of 5 speakers (Monacor MKS-26/SW, MONACOR International GmbH & Co. KG, Bremen, Germany) which were located at 5 horizontal locations (-17°, -8.5°, 0°, 8.5°, 17°, vertical midline = 0°; Figure 1). Sound presentation was controlled via a multi-channel soundcard (Creative Sound Blaster Z) and amplified via an audio amplifier (t.amp E4-130, Thomann Germany). Visual stimuli were projected (Acer Predator Z650, Acer Inc., New Taipei City, Taiwan) onto an acoustically transparent screen (Screen International Modigliani, 2x1 m), which was located at 135 cm in front of the participant. The visual stimulus was a cloud of white dots distributed according to a two-dimensional Gaussian distribution (N = 200, SD of vertical and horizontal spread 2°, width of a single dot = 0.12°, duration = 50 ms). Stimulus presentation was controlled using the Psychophysics toolbox (Brainard, 1997) for MATLAB (The MathWorks Inc., Natick, MA) with ensured temporal synchronization of auditory and visual stimuli.

2.3. Experimental Setup

The paradigm was based on a single-trial audio-visual localization task (Park and Kayser, 2019; D. R. Wozny and Shams, 2011), with trials and conditions designed to probe both the ventriloquist effect and the ventriloquist aftereffect. Participants were seated in front of an acoustically transparent screen, with their heads on a chin rest. Five speakers were located immediately behind the screen. Participants responded with a mouse cursor (Figure 1A).

The participants' task was to localize a sound during either Audio-Visual (AV) or Auditory (A), trials, or to localize a visual stimulus during few Visual (V) trials. The locations of auditory and visual stimuli were drawn semi-independently from the 5 locations to yield 9 different audio-visual discrepancies (abbreviated ΔVA in the following; -34°, -25.5°, -17°, -8.5°, 0°, 8.5°, 17°, 25.5°, 34°). We repeated each discrepancy between the locations of auditory and visual stimuli 44 times for YA, 45 times for OA, resulting in a total of 396 AV-A trial pairs for YA, and 405 for OA (except for the first OA who did the same amount as the YA (hence 396 pairs), and one OA for which one block was lost, resulting in 324 pairs). In addition, on average 72 and 65 visual-only trials were interleaved to maintain attention (V trials always came after A trials, thus not interrupting the AV-A sequence), for the YA and OA respectively, resulting in a total of 864 trials for YA and 875 trials for OA. Trials were pseudo-randomized and divided into 4 blocks for YA and 5 blocks for OA. Each trial started with a fixation period (uniform 700 ms – 1100 ms), followed by the stimulus (50 ms). After a random post-stimulus period (uniform 400 ms - 700 ms) the response cue emerged, which was a horizontal bar along which participants could move a cursor. A letter 'T' was displayed on the cursor for 'tone' in the AV or A trials, and 'V' for the V trials to indicate which stimulus participants had to localize. There was no constraint on response times. Inter-trial intervals varied randomly (uniform 900 ms - 1200 ms). A typical sequence of trials is depicted in Figure 1B. Participants were asked to maintain fixation during the entire trial except the response, during which they could freely move their eyes.

All participants underwent a test for spatial hearing prior to the main study. We used four of the five potential sound locations (excluding the middle one) and asked participants to indicate the perceived location by pressing left or right keys on a keyboard (2-AFC procedure). The median accuracy across all four sound positions for YA was 97.5% (range: 85.0% ~ 100%) and 92.5% (range: 72.5% ~ 100%) for OA, indicating they could localize the sounds well. We compared the thresholds (at 50% correct) and slopes obtained from psychometric fits (fitted with a logistic function, free but equal lapse and guess rates) (psignifit toolbox version 4) between groups: the thresholds were 1.09° ± 2.56°, 1.00° ± 4.05° (mean ± SD) for the YA and OA respectively, and the slopes 0.074 ± 0.018 and 0.052 ± 0.023, respectively. A Wilcoxon rank sum test showed no difference for thresholds ($p = 0.9112$, z value = 0.111), but indicated significantly different slopes ($p = 0.01$, z value = 2.77, corrected for multiple comparisons with the Holm method), suggesting that YA were more sensitive to auditor spatial information than OA.

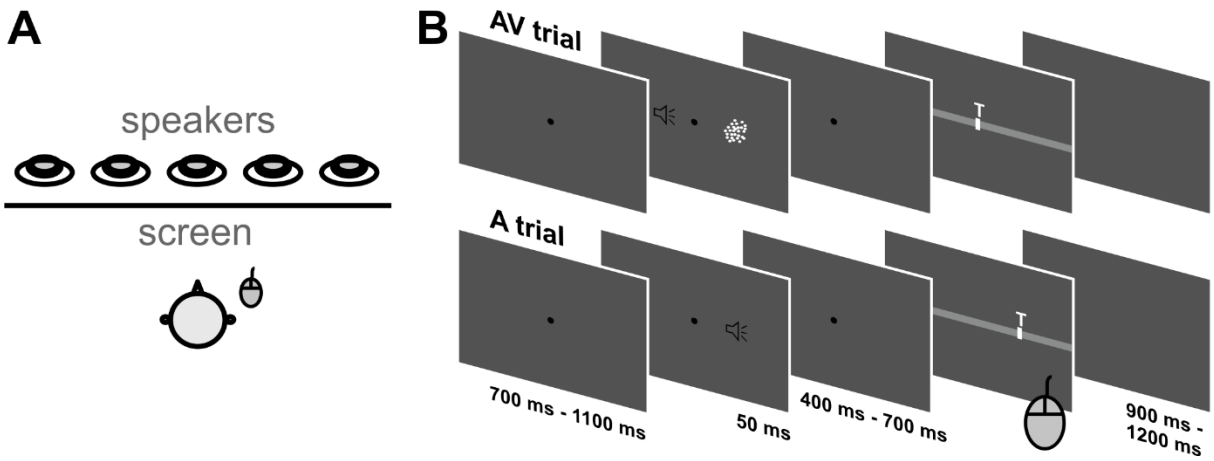

Figure 1. Experimental setup and task. (A) Top view of the experimental setup. **(B)** Time-course of the sequence of AV and A trials (infrequent V trials are not shown). The black speaker icons are for display purposes only. The A trial always followed the AV trial, and participants responded using a mouse cursor.

2.4. Analysis of behavioral biases

We quantified the perceptual biases observed in the AV and A trial as follows. The single-trial Ventriloquist effect (ve) was defined as the bias induced by the visual stimulus away from the true sound location in the AV trial: i.e. the difference between the reported sound location (R_{AV}) and the location at which the sound (A_{AV}) was actually presented (ve = R_{AV} - A_{AV}). Then, the overall VE-bias for each participant was defined as the regression slope of ve against the audio-visual discrepancy (ΔVA).

The Ventriloquist after-effect was defined as the bias in the reported sound location in the auditory trial relative to the audio-visual discrepancy experienced in the previous trial. The single-trial Ventriloquist after-effect (vae) was computed as the difference between the reported sound location (R_A) and the mean reported location for all A trials of the same stimulus position (μ_{RA}), i.e., (vae = R_A - μ_{RA}). This was done to ensure that any overall bias in sound localization (e.g. the tendency to perceive sounds closer to the midline than they actually are) would not influence this measure (D. R. Wozny and Shams, 2011). Then the overall VAE-bias was quantified as the slope of vae against ΔVA for each participant.

To understand the main causes of these response biases we modelled the single trial responses using general linear models. We compared three models as potential explanation of the response in the AV trial, based on either just a single unisensory stimulus or their combination: mAV_1: $R_{AV} \sim 1 + A_{AV}$, mAV_2: $R_{AV} \sim 1 + V_{AV}$, mAV_3: $R_{AV} \sim 1 + A_{AV} + V_{AV}$. For the A trial we compared different models predicting the

response based on either the previous audio-visual discrepancy (ΔVA) or the previous response (R_{AV}): mA_1; $R_A \sim 1 + A_A + \Delta VA$, mA_2; $R_A \sim 1 + A_A + R_{AV}$. See (Park and Kayser, 2019) for a similar approach.

To quantify to what degree the single trial recalibration (vae) is directly related to the integration (ve) of audio-visual information in the previous trial, we probed whether the strength of the trial-by-trial association of the respective biases (ve,vae) is related to the participant-average (VE or VAE) bias. To this end we computed two correlations: first, for each participant the trial-wise correlation of ve and vae as a measure of the trial-wise link between multisensory integration and subsequent recalibration (termed 'cvv', based on Pearson correlation); and second, the between-participant correlation of this ccv index with the VE-bias and VAE-bias (Spearman rank correlations).

2.4.1. *Reaction times (RT)*

RTs were obtained when participants clicked with the mouse to indicate the perceived spatial location. RTs hence included both perceptual decision times and motor noise. Still, to obtain an overall measure of response speed, we compared the participant-averaged RTs between groups and trial types (AV, A).

2.5. Statistical Analysis

Behavioral biases were tested against zero using two-sided Wilcoxon signed rank tests, corrected for multiple tests using the Holm procedure with a FWE of p = 0.05. Behavioral biases between groups were tested with the Wilcoxon rank sum test for equal medians (corrected using the Holm procedure with a FWE of p = 0.05). General linear models were fit using maximum-likelihood procedures (fitglme.m in MATLAB). The Scheirer–Ray–Hare test (Sokal and Rohlf, 1981) was used to test for a non-parametric Group x Trial type (A trial or AV trial) interaction for the bias standard deviations and reaction times.

2.6. Model-based Analyses

2.6.1. Bayesian Causal Inference Model of Integration

In order to investigate which aspect of underlying sensory computations is affected by aging, we modelled the behavioral data using Bayesian causal inference (BCI) models with different potential decision strategies. These models have been shown to capture the computations underlying flexible multisensory perception well (Cao et al., 2019; Körding et al., 2007; Rohe et al., 2019; Rohe and Noppeney, 2015a; Wozny et al., 2010). Briefly, the BCI model reflects the inference process about the true causal relations of two sensory-motor features based on prior experience and the available sensory

evidence. Specifically, the model predicts the belief in a single (C=1) or two distinct (C=2) causes giving rise to two noisy sensory inputs, x_V, x_A, as follows:

$$p(C|x_V, x_A) = \frac{p(x_V, x_A|C)P_{COM}}{p(x_V, x_A)} \qquad \text{(eq. 1)}$$

Here, P_{COM} denotes the a priori tendency of an observer to belief in a common source of two sensory items. Under the assumption of two separate causes, the optimal estimates of the unisensory sensory locations (Körding et al., 2007):

$$\hat{s}_{A,C=2} = \frac{\frac{x_A}{\sigma_A^2} + \frac{\mu_P}{\sigma_P^2}}{\frac{1}{\sigma_A^2} + \frac{1}{\sigma_P^2}}, \qquad \hat{s}_{V,C=2} = \frac{\frac{x_V}{\sigma_V^2} + \frac{\mu_P}{\sigma_P^2}}{\frac{1}{\sigma_V^2} + \frac{1}{\sigma_P^2}} \qquad \text{(eq. 2)}$$

And under the assumption of a common cause they are given by the linear weighted average (Ernst and Banks, 2002):

$$\hat{s}_{A,C=1} = \hat{s}_{V,C=1} = \frac{\frac{x_A}{\sigma_A^2} + \frac{x_V}{\sigma_V^2} + \frac{\mu_P}{\sigma_P^2}}{\frac{1}{\sigma_A^2} + \frac{1}{\sigma_V^2} + \frac{1}{\sigma_P^2}} \qquad \text{(eq. 3)}$$

Here $\hat{s}_{i,C=j}$ is the estimate for the visual $i = V$ or the auditory $i = A$ stimulus location based on the sensory sample x_i. We modelled sensory representations (likelihoods) using Gaussian distributions around the true location, with standard deviation σ, and the true sensory location μ . We allowed for an overall bias in spatial perception (Cao et al., 2019; Körding et al., 2007; Rohe and Noppeney, 2015a; Wozny et al., 2010), modelled as Gaussian distribution with mean μ_P and standard deviation σ_P.

In this model, the observer derives a final estimate about the stimulus location after obtaining the posterior probabilities about the possible causal scenarios and using a specific decision strategy. We considered three frequently studied strategies (Cao et al., 2019; Körding et al., 2007; Rohe and Noppeney, 2015a; Wozny et al., 2010): Model Averaging (MA), Model Selection (MS), and Probability Matching (PM). With the MA strategy, the final estimate is derived by the weighted-average of the two estimates derived under each causal relation:

$$\hat{s}_A = p(C = 1|x_V, x_A)\hat{s}_{A,C=1} + \big(1 - p(C = 1|x_V, x_A)\big)\hat{s}_{A,C=2} \qquad \text{(eq. 4)}$$

The MA strategy minimizes the mean expected squared error of the spatial estimates (Körding et al., 2007; Wozny et al., 2010).

The MS strategy uses the posterior probability to guide the decision by choosing the estimate associated with the causal structure of higher probability:

$$\hat{s}_A = \begin{cases} \hat{s}_{A,C=1} & \text{if} \quad p(C=1|x_V, x_A) > 0.5 \\ \hat{s}_{A,C=2} & \text{if} \quad p(C=1|x_V, x_A) \leq 0.5 \end{cases} \qquad \text{(eq. 5)}$$

Finally, PM strategy uses a stochastic selection criterion, by choosing a causal scenario in proportion to its posterior probability, which can be implemented by sampling a random ξ from a uniform distribution on each trial:

$$\hat{s}_A = \begin{cases} \hat{s}_{A,C=1} & \text{if} \quad p(C=1|x_V, x_A) > \xi \\ \hat{s}_{A,C=2} & \text{if} \quad p(C=1|x_V, x_A) \leq \xi \\ \text{where } \xi \in [0:1] \text{ uniform distribution,} & \\ \text{sampled on each trial} & \end{cases} \qquad \text{(eq. 6)}$$

2.6.2. Bayesian Causal Inference Model of Recalibration

To model the ventriloquist after-effect observed for the sound localization during the A trials we derived a novel version of the BCI model, by combining relevant features from both the previous (AV) and the current (A) trial. We hypothesized that the perceptual bias arising from the audio-visual integration during the AV trial persists during the next trial, and is combined with the acoustic information in proportion to a belief that the previous and current trial are causally linked. To allow for different sensory or motor features as causes for the VAE (see above), we considered different versions of this between-trial BCI model that combined either the previous sensory experience or the previous motor response with the current acoustic information. The posterior probability for a causal association of the audio-visual and auditory trials is:

$$p(C_T|x_{AV}, x_A) = \frac{p(x_{AV}, x_A|C_T)P_{COMT}}{p(x_{AV}, x_A)} \qquad \text{(eq. 7)}$$

Whereby C_T = 1 indicates that the previous and current trial are linked, and C_T = 2 indicates they are separate entities. x_{AV} denotes the previous experience: this could be either the previous response

R_{AV}, or the influence of the previous audio-visual discrepancy on the current acoustic information, $x_A + \Delta VA$. By using the sum of the audio-visual discrepancy ΔVA and the current sound location x_A we ensured that the same spatial dimension was used for both versions of the model. Here P_{COMT} reflects the tendency to combine the previous experience with the current evidence. The estimates derived under the two causal scenarios were then derived similar as in equations 2 and 3.

For the VAE we considered model averaging as the only decision strategy. The reason was that the response in the auditory trial R_A is always in large determined by the current sound, with the previous trial adding only a proportionally small bias. In contrast to this, the MS or PM decision strategies would allow for trials with responses determined solely based on the previous experience and ignoring the current acoustic information, which seems at odds with the behavioral data on the VAE.

2.6.3. Model Fitting

We optimized model parameters using the BADS toolbox based on the log-likelihood of the true data under the model (Bayesian Adaptive Direct Search (v1.0.3) (Acerbi and Ma, 2017). Each model (MA, MS, and PM for integration, bΔVA and bR_{AV} for recalibration) had 5 free parameters: σ_A, σ_V ($\sigma_{\Delta VA}$ or σ_{RVA} for the recalibration model), σ_P, P_{COM} (P_{COMT}), and μ_P. We repeated the fitting procedure 500 times using different starting values. For each run, we produced 20,000 simulations for true stimulus location ($\hat{s}$) for each model and binned the distributions of real and simulated data into 73 bins (-36° to 36°, increment = 1°). For the recalibration model, the true stimulus locations were the 9 ΔVA values when considering bΔVA as predictor, and the 9 mean values from each of the equi-populated bins of the response in the AV trial (R_{AV}) when considering bR_{AV}. The log-likelihood of the actual data was derived from the overlap of real and simulated counts per bin, under the assumption that the different conditions were statistically independent. The best parameters for each model and participant was obtained as the mean of the parameters from the three best runs. Group-level BIC values were obtained by assuming that individual participants provided independent data.

2.6.4. Model Comparison

To compare the predictive power of different regression models, we calculated the log-evidence of each model and obtained the corresponding BIC values. Based on the BIC we computed protected exceedance probabilities using the VBA-toolbox (Rigoux et al., 2014). For the Bayesian model analysis, we derived the BIC from the log-likelihood obtained from the best model fits. Using -0.5·BIC as model

evidence, we calculated the protected exceedance probabilities. The best model for each participant was chosen as the model with the lowest BIC.

2.6.5. Recovery of behavioral biases from model simulations

We simulated the predicted behavioral responses from the obtained model parameters from both the VE and VAE CI models for each participant to ensure the model indeed captures the behavioral data (Palminteri et al., 2017). We simulated 10,000 trials based on the exact stimuli presented to each participant using equations 2,3,8, and 9. We then calculated the mean VE-bias and VAE-bias across the simulated trials, deriving a prediction of the average bias under each specific model and participant specific parameters (Figure 2).

3. RESULTS

3.1. Biases in multisensory perception

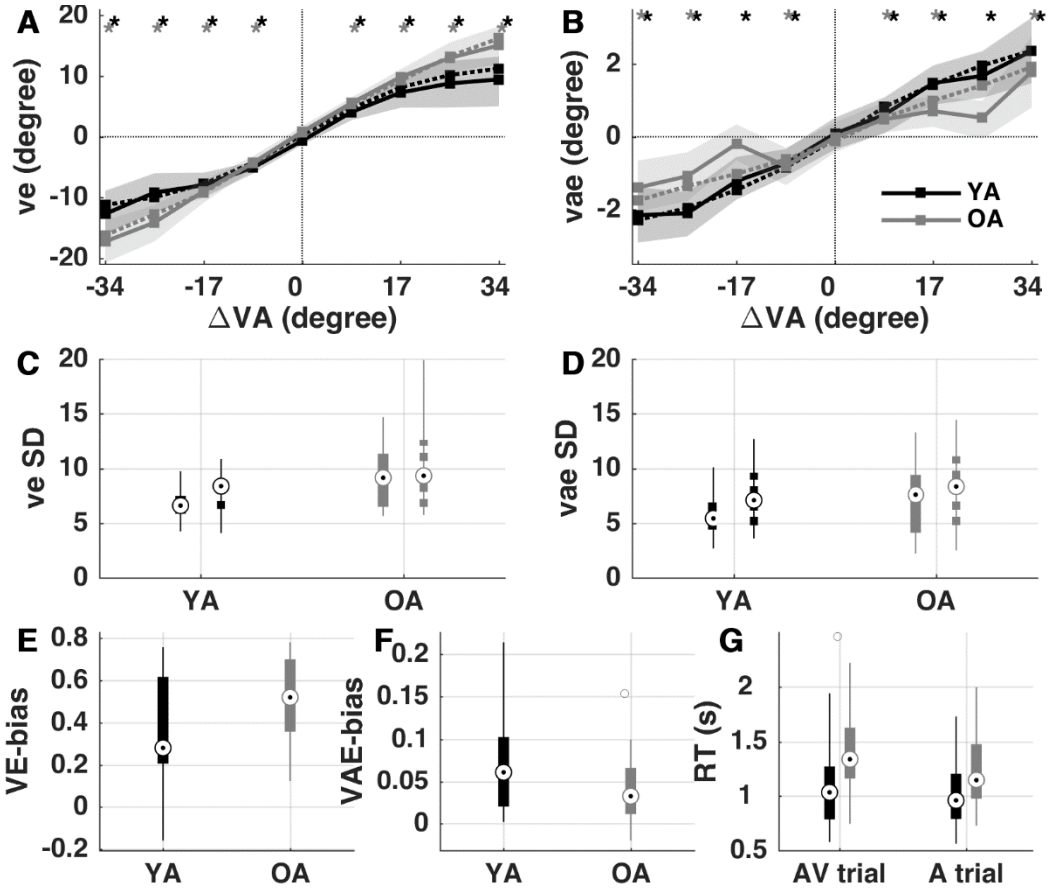

Figure 2. Ventriloquist biases. (A) The Ventriloquist bias (ve = R_{AV} - A_{AV}), **(B)** the Ventriloquist aftereffect bias (vae = R_A - μ_{RA}) as a function of the audio-visual discrepancy (ΔVA) **(A-B)** solid lines indicate the mean of the actual data, shaded areas the 95% bootstrap confidence interval of the mean, and dotted lines are mean bias predicted by the BCI model. Asterisks denote significant difference from zero bias (two-sided Wilcoxon signed rank tests, corrected for multiple tests using the Holm procedure with a FWE of p = 0.05). **(C-D)** Boxplots of the respective standard deviation of these biases averaged across ΔVA. Dotted boxes are predicted standard deviations by the BCI model. **(E-F)** Box plots of regression slopes predicting the ve (A) and vae (B) as a function of ΔVA. **(G)** Box plots of reaction times (RT). In all panels, black and grey denote YA and OA participants, respectively.

Figure 2A, B shows the response biases for audio-visual integration (ve) and the trial by trial aftereffect (vae). The magnitudes of biases were all significantly larger than zero (two-sided Wilcoxon signed rank tests, corrected for multiple tests using the Holm procedure with a FWE of p = 0.05) for nearly all non-zero discrepancies (ΔVA) for both groups (c.f. Figure 2A-B). The average strength of neither bias,

quantified as regression slope of ve (vae) against the multisensory discrepancy (Figure 2E-F), differed between groups. The VE effect sizes were 0.36 ± 0.28 (mean ± SD) for YA and 0.51 ± 0.19 for the OA. The VAE effect sizes were 0.07 ± 0.06 (mean ± SD) for YA and 0.04 ± 0.04 for the OA. A Wilcoxon rank sum test did not provide evidence for any significant group-level difference ($p = 0.15$, $Z = -1.79$ for both biases, corrected for multiple comparisons with the Holm method; c.f. Figure 2E-F and Table 1 for details and uncorrected p-values), speaking against a change of multisensory perceptual biases with age.

3.2. *Increased variability in perceptual bias in the OA*

We quantified the trial-by-trial variability of the ve/vae biases to compare the within-participant consistency of these between groups. As the data (Figure 2C) suggested also a difference between multisensory (AV) and unisensory trials (A), we tested for effects of both group and trial-type using a non-parametric two-way ANOVA (Scheirer-Ray-Hare test). This indicated a group difference ($H = 9.78$, d.f. = 1, $p = 0.0018$), and a Trial Type difference ($H = 5.74$, d.f. = 1, $p = 0.017$), but no Group x Trial interaction ($H = 0.1131$, d.f. = 1, $p = 0.737$), showing that the perceptual biases for the OA were more variable, and more pronounced in the presence of a multisensory distractor for both groups (Figure 2C-D, Table 1).

3.3. Reaction time

Although the nature of the obtained reaction times (RT) does not distinguish between motor-related factors and the perceptual-decision, we used these to confirm that the OA generally responded slower than the YA. A non-parametric ANOVA confirmed a group difference (SRH test: $H = 12.3$, d.f. = 1, $p = 0.0005$) with no Group x Trial Type interactions ($H = 0.389$, d.f. = 1, $p = 0.533$).

Table 1. Summary of the behavioral data. YA: younger adults, OA: older adults. VE/VAE-bias: regression slopes of ve/vae against ΔVA. VE/VAE SD: VE/VAE standard deviation for each participant averaged across ΔVA. SRH: Scheirer-Ray-Hare test (H statistic). d.f.: degrees of freedom.

	YA		OA		Wilcoxon's test (between groups G) p-value z-value
	Slope vs ΔVA.				
	Median	Conf. Int.	Median	Conf. Int.	
VE-bias	0.281	[-0.023, 0.343]	0.520	[0.403, 0.680]	0.0741 -1.79
VAE-bias	0.0611	[0.024, 0.090]	0.0324	[-0.0007, 0.0511]	0.0741 -1.79
					SRH ANOVA (Group, Group x trial type)
VE SD	6.61	[5.88, 7.14]	9.15	[7.18, 11.6]	H = 9.78, d.f. = 1, p = 0.0018
VAE SD	5.43	[4.00, 6.38]	7.60	[6.12, 10.9]	H = 0.113, d.f. = 1, p = 0.737
	Reaction Time (s)				SRH ANOVA (Group, Group x trial type)
AV trial	1.03	[0.825, 1.25]	1.34	[1.11, 1.50]	H = 12.3, d.f. = 1, p = 0.0005
A trial	0.96	[0.816, 1.11]	1.15	[0.938, 1.30]	H = 0.389, d.f. = 1, p = 0.533

3.4. Modelling the Ventriloquist effect

First, we tested linear models predicting the response in the AV trial, R_{AV}, based on auditory and visual stimulus locations. For both groups we confirmed that the R_{AV} was shaped by both the auditory and visual stimuli, as expected. In both groups the comparison of regression models identified the multisensory model (mAV_3; c.f. Materials and Methods) as winning model (relative group-level BIC for YA: [mAV_1, mAV_2, mAV_3] = [2379, 6173, 0]; OA: [mAV_1, mAV_2, mAV_3] = [2137, 1638, 0]).

Second, we fit Bayesian causal inference models (VE CI; c.f. Methods) to individual participant's data. To assess the quality of the model fit we calculated the explained variance across conditions. The

participant-specific best-fitting models explained the data well (YA: [MA, MS, PM] = [95.5%, 95.0%, 95.4%]; OA: [MA, MS, PM] = [86.8%, 85.6%, 86.6%]). The comparable quality of fit between groups is also borne out in the normalized (by number of samples) negative log-likelihoods, which were comparable between groups (YA: [MA, MS, PM] = [3.39, 3.36, 3.36] and OA: [MA, MS, PM] = [3.16, 3.15, 3.12]).

Interestingly, the decision-strategies best explaining the observed data differed between groups. In the YA, models based on the PM strategy explained the group-level data best, while in the OA, models based on the MS strategy provided the overall best group-level fit (relative summed-BIC values [MA, MS, PM] = [640, 419, 0] for YA; [MA, MS, PM] = [491, 0, 38] for OA; c.f. Figure 3A, left). While the group-level BIC differences between models provided decisive evidence for a difference, we note that an assessment based on exceedance probabilities provided no conclusive picture ([0.28, 0.34, 0.38] for YA; [0.20, 0.59, 0.21] for OA; Figure 3A, right).

Comparing the model parameters of the participant-specific best-fitting models between groups revealed a significantly reduced sensory precision for auditory and visual spatial information in the OA (Figure 3B; Table 2). The other model parameters did not differ. With regards to our main questions these data show that overall the same class of sensory computations (i.e. the BCI models) can explain the VE bias for both groups. While there seem to be differences in the prevalence of individual decision strategies between groups, the a priori belief that the auditory and visual stimuli are causally linked (P_{COM}) did not differ (Table 2). Hence, both groups tended to combine the audio-visual evidence to the same degree.

We confirmed that the model not only reproduces the mean bias for individual participants (Figure 2A-B), but also verified that the model and the different parameter regimes for YA and OA indeed account for the increased trial-by-trial variability of the bias (c.f. Figure 2C-D). More detailed model simulations confirmed that the increased variability in the OA likely results from the reduced reliability of the uni-sensory representations rather than the difference in preference of decision-making strategy. Specifically, we simulated models with the median parameters from the YA and OA groups and compared the trial-by-trial variability across parameters (YA and OA) and decision functions (MS and PM). This showed that changing the decision function (MS and PM) only produced a moderate change in VE SD, while changing the parameters from YA to OA produced a twice as large change in the VE

SD, suggesting that the higher trial-by-trial variability in the OA results mostly from the associated changes in sensory precision.

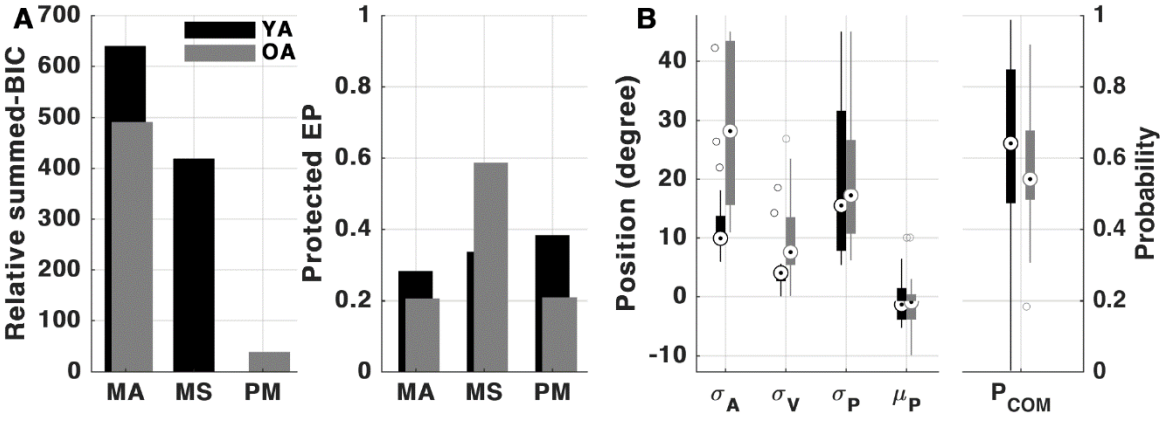

Figure 3. Modelling the VE using causal inference. (A) Relative group-level BIC values (left), protected exceedance probabilities (EP) (right). **(B)** Model parameters. Black circles denote the median, and the bars are the 25% and 75% percentiles. In both panels, black and grey indicate YA and OA, respectively.

Table 2. Model parameters of participant-specific best-fitting VE CI model. YA: younger adults, OA: older adults. σ_A: standard deviation of the auditory likelihood, σ_V: standard deviation of visual likelihood, σ_P: standard deviation of prior, μ_P: mean of prior, P_{COM}: a priori binding tendency. *corrected for multiple comparisons with Holm's method.

	YA		OA		Wilcoxon's test (between groups)
	Median	Conf. Int.	Median	Conf. Int.	p-value* z-value
σ_A	9.86	[8.45, 10.6]	28.1	[21.9, 39.6]	**0.0001** **-4.36**
σ_V	4.02	[3.08, 5.37]	7.53	[-1.83, 9.39]	**0.0160** **-2.88**
σ_P	15.4	[8.50, 22.6]	17.2	[8.916, 22.1]	1.0000 -0.52
μ_P	-1.34	[-3.47, 0.71]	-0.901	[-1.83, 1.61]	1.0000 0.45
P_{COM}	0.641	[0.443, 0.795]	0.541	[0.499, 0.601]	0.8068 1.11

3.5. Modelling the Ventriloquist aftereffect

Our modelling analyses suggest that the factors driving the recalibration effect differed between groups. First, in a first (linear) analysis, we used GLMs to probe whether the response in the A trial is better explained by the multisensory discrepancy in the preceding audio-visual trial (mA_1), or the participant's response in that trial (mA_2) (Park and Kayser, 2019). A comparison of both GLMs (c.f. Methods) revealed that the model based on the previous sensory information better explained the response in the YA, while the model based on the previous response better explained the response in the OA (relative group-level BIC for [mA_1; mA_2] = [0, 437] for YA, and [214, 0] for OA; protected exceedance probabilities [0.92, 0.08] for YA, and [0.37, 0.63] for OA).

In a second analysis we fit a modified Bayesian causal inference model to the trial-by-trial recalibration data (cf. Methods). This VAE CI model explained the data in both groups well and the quality of model fit was comparable between groups (explained variance: YA: [$b\Delta VA$; bR_{AV}] = [96.0%, 95.6%]; OA: [90.3%, 89.0%]; normalized negative log-likelihoods: YA: [3.33, 3.34]; OA: [3.35, 3.33]).

The comparison of candidate VAE CI models confirmed the above result that in the YA the response in the A trial was better explained by the previous multisensory discrepancy (ΔVA), whereas in the OA it was better explained by the previous response (R_{AV}). The overall quality of model fit based on the group-level BIC value provided highly conclusive evidence in favour of distinct models in each group (YA: [bΔVA; bR_{AV}] = [0, 123]; OA: [355, 0]; Figure 4B) while a comparison based on protected exceedance probabilities yielded less conclusive evidence (YA: [0.62, 0.38]; OA [0.49, 0.51]).

The parameters for the participant-specific best-fitting models are shown in Figure 4C. Again we found group-difference in the precision of the unisensory auditory representation (σ_A; c.f. Table 3), in line with the results on the VE above. Also the central bias (μ_P) differed between groups, suggesting a somewhat stronger spatial lateralization bias in the YA. Importantly, and similar as for the ventriloquist effect, the a priori belief into an association of the two trials (P_{COMT}) did not differ (Table 3).

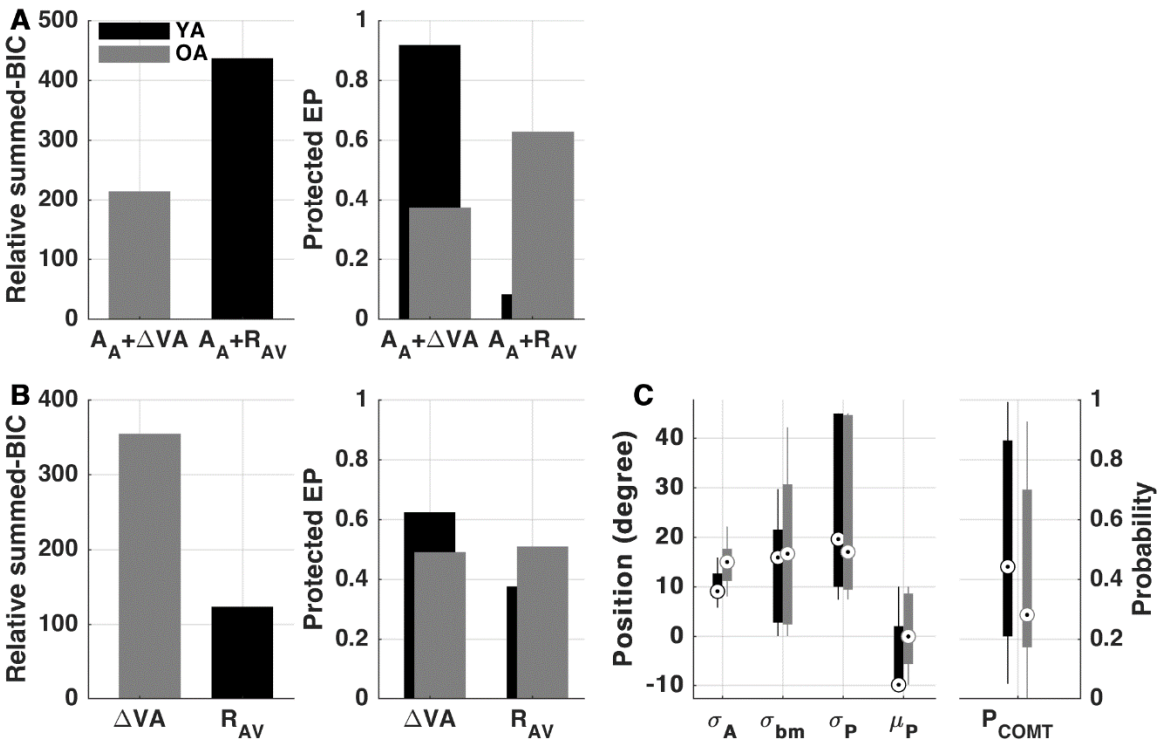

Figure 4. Model-based analysis of the VAE. (A) Linear regression models (mA_1, mA_2), relative Summed-BIC (left), Protected EP (right). **(B)** VE CI model (bΔVA, bR_{AV}), relative Summed-BIC (left), Protected EP (right). **(C)** Parameters for the best model for each participant. 'bm' for the second parameter denotes 'best model', since the parameters were chosen for the participant-wise best model (either bΔVA or bR_{AV}) based on the BIC. Black circle dots are the median values, and the bars are the 25% and 75% percentiles. In all panels, black and grey indicate YA and OA, respectively.

Table 3. Model parameters of the participant-specific best-fitting VAE CI model. YA: younger adults, OA: older adults. σ_A: standard deviation of auditory likelihood, σ_V: standard deviation of visual likelihood, σ_P: standard deviation of prior, μ_P: mean of prior, P_{COMT}: a priori binding tendency. *corrected for multiple comparisons with Holm's method.

	YA			OA			Wilcoxon's test (between groups)
	Median	Conf. Int.		Median	Conf. Int.		p-value* Z-value Rank sum stats
σ_A	9.06	7.41	10.2	15.0	12.5	17.5	**0.0013** **-3.65**
σ_{bm}	15.9	10.4	28.6	16.6	8.23	30.7	1.0000 -0.67
σ_P	19.6	-5.79	27.9	17.0	-3.97	22.8	1.0000 0.33
μ_P	-9.93	-18.7	-9.85	-0.0584	-6.70	4.79	**0.0233** **-2.76**
P_{COMT}	0.442	0.0691	0.620	0.281	0.0608	0.389	0.487 1.40

3.6. Qualitative validation of model parameters

We confirmed the validity of the participant-specific best-fitting BCI models by further relating model parameters to the behavioral data.

First, we confirmed that the P_{COM} variable, i.e., the tendency to bind the visual and acoustic stimuli during the VE, indeed predicts the strength of the participant specific VE-bias (derived in Figure 2C). For both groups, P_{COM} and the overall VE-bias were significantly correlated (Spearman's correlation for YA: Rho = 0.70, p = 0.0006, CI = [0.38, 0.89]; OA: Rho = 0.56, p = 0.0081, CI = [0.16, 0.84], corrected for multiple comparisons with the Holm method, CI based on bootstrapping). Second, we confirmed that the P_{COMT} in the VAE CI model, hence the tendency to associate the two trials, indeed predicts a stronger VAE-bias resulting from the influence of the AV onto the A trial. For both groups, the P_{COMT} variable was significantly correlated with the overall VAE-bias (defined against the ΔVA or binned R_{AV}, for respective models, cf. Methods, 'Model Fitting') (Spearman correlation for YA: Rho = 0.66, p = 0.0018, CI = [0.35,

0.84]; OA: Rho = 0.55, p = 0.0097, CI = [0.14, 0.79], corrected for multiple comparisons with the Holm method, CI based on bootstrapping).

3.7. The tendency to combine evidence across trials is linked to the overall biases

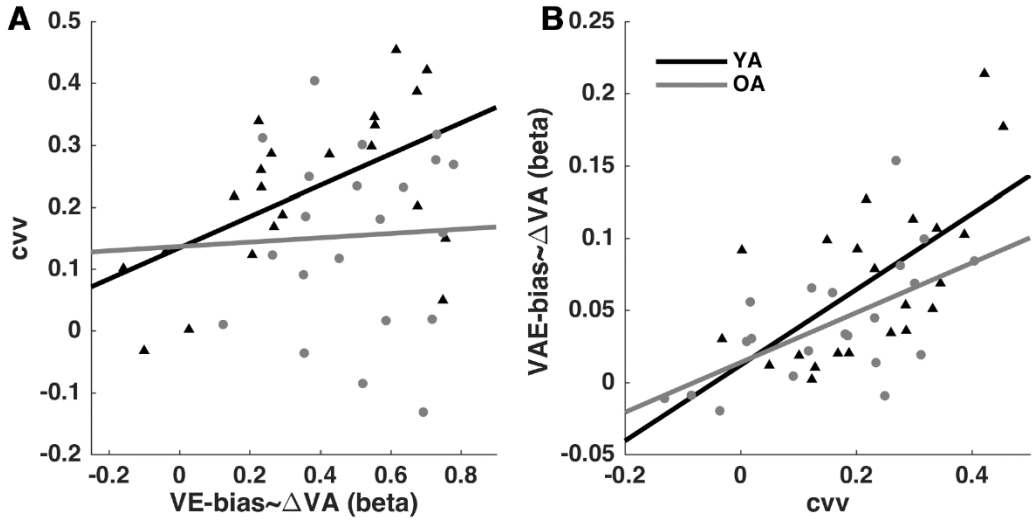

Figure 5. Single-trial ve/vae coupling (cvv) and the overall biases. (A) Correlation (Spearman rank) between participant-wise VE-bias and the single trial coupling (cvv). **(B)** Correlation between participant-wise VAE-bias and trial-wise coupling (cvv). In both panels, black triangles and grey circles indicate YA and OA, respectively. Solid lines are linear regression lines for each group.

The above modelling results suggest a mechanistic link between the AV trial (stimulus, or response) and the subsequent response bias in the A trial. To directly capture this single-trial link, we derived an index of this trial-wise coupling by computing the participant-specific correlation between the single-trial ve and vae biases (termed ‘cvv’). This trial-wise coupling was significant for 19 out of 22 participants in the YA, and 15 out of 21 in the OA (at $p < 0.05$). Numerically the average link was larger for the YA than the OA (average correlation coefficients 0.224 and 0.154 for YA and OA), and a permutation test suggested that the difference approaches significance (10000 permutations of group-labels, p = 0.0517).

We then used this index of single-trial link (cvv) to further explore the group-differences in how the VAE is related to the multisensory discrepancy experienced during the AV trial. For the YA, the above modelling results suggest that the vae is directly driven by the multisensory discrepancy, hence predicting a correlation between the amount of cvv and the participant-specific VAE-bias: this was indeed confirmed (rho = 0.66, p = 0.0009, CI = [0.30 0.86]). Furthermore, if the strength of multisensory

integration in the AV trial determines the vae, one should also expect a correlation between the participant-specific VE-bias and the cvv: this was also confirmed (rho = 0.47, p = 0.0276, CI = [-0.03 0.85]).

For the OA, the modelling results suggest that the vae is driven by the experience in the previous trial. Hence, also in this group the cvv should be related to the participant-specific VAE-bias, which we confirmed (rho = 0.61, p = 0.0031, CI = [0.20 0.86]). However, in the OA the after-effect was driven by the previous response, rather than the audio-visual discrepancy. Hence, we expected the correlation between the VE-bias and the single-trial link to be weak, which was indeed the case (rho = 0.13, p = 0.5825, CI = [-0.37 0.55]). Overall this supports the conclusion that in both groups the overall response bias in the A trial is related to the correlation of response biases between trials. But only in the YA this trial-wise bias correlation is driven by the previous multisensory discrepancy, while in the OA it is driven by their previous motor response.

4. DISCUSSION

While previous studies described multiple changes in multisensory perception with age, the precise origin of these remained unclear. We used a model-based approach to characterize and disentangle age-related changes at four levels of the sensory decision process: the precision of uni-sensory representations, the a priori belief that two items of sensory-motor information are causally linked, the decision rules used to forge sensory estimates derived from different causal models, and the overall ability of the same computational architectures to account for the behavioral data of younger and older participants. Our data show that both the strength of the ventriloquist bias and its after-effect are comparable between groups, and can be explained by the same class of computational models, albeit with differences in the prevalence of different decision strategies. However, the OA exhibited a significantly reduced auditory precision, and in contrast to the YA, their ventriloquist aftereffect (VAE) was not driven by the previous sensory information but rather by their previous response. Thereby our results point to a profound change in the nature of trial-by-trial perceptual dependencies underlying preserved multisensory capacities.

4.1. Perseverance in multisensory perception with age

A number of changes in multisensory perception with age have been reported. For example, OA benefit more from multisensory compared to unisensory information during speeded detections (Laurienti et al., 2006; Mahoney et al., 2014; Zou et al., 2017), OA have longer multisensory temporal binding windows (Chan et al., 2014a; DeLoss et al., 2013; Hay-McCutcheon et al., 2009), OA experience increased difficulty to separate distinct multisensory events compared to YA (Setti et al., 2011), and experience stronger a McGurk effect (Sekiyama et al., 2014; Setti et al., 2013). Similar age-effects have also been reported in the context of multisensory recalibration (Buch, 2003; Chan et al., 2014b), where OA show reduced adaptation. Contrasting this view, recent work suggests that the healthy young and aging brains may follow similar rules when combining multisensory information (Billino and Drewing, 2018; Campos et al., 2018; Cressman et al., 2010), except possibly that that OA may take longer to respond (Jones et al., 2019. see also Smith & Brewer, 1995; Starns & Ratcliff, 2010).

Supporting this notion of a preserved multisensory capacity in the elderly we found similar response biases during multisensory integration and recalibration in young and elderly participants. This preserved multisensory capacity in the OA is reflected in two key findings. First, the behavioral data in both the VE and VAE conditions can be explained by the same class of perceptual models in both

groups, suggesting that the qualitative computations underlying multisensory perception are preserved with age. Second, the a priori belief about a common source underlying the audio-visual information during integration, and the belief about a causal association between trials during the after-effect, did not differ between groups. This suggests that the overall tendency to combine sensory attributes in a ventriloquist setting are not affected by aging.

4.2. Changes in multisensory decision making with age

In line with previous work we found that the pattern of audio-visual integration during the VE can be described using Bayesian causal inference (Körding et al., 2007; Rohe and Noppeney, 2015b; Wozny et al., 2010). The typical BCI models considered in the literature comprise a number of decision strategies to combine the sensory evidence derived under the assumption of a single or two distinct causes giving rise to two stimuli (Körding et al., 2007; Rohe and Noppeney, 2015a; Wozny et al., 2010). We found that the decision strategy best explaining the group-level data differed between groups: for the YA probability matching provided the best group-level fit, in line with previous studies on spatial perception (Wozny et al., 2010; David R. Wozny and Shams, 2011).

To our knowledge no previous study has compared different putative decision strategies for multisensory integration in the elderly. In the present data the model selection strategy provided the best group-level fit for the OA, suggesting that the processes and behavioral strategies converting multisensory evidence to an overt response may change with age (Dully et al., 2018). Still, further studies are required to corroborate such a shift in decision strategies and to relate changes in multisensory decision processes to possibly more general changes in cognitive strategies with age (Dully et al., 2018; Koen and Rugg, 2019; Nyberg et al., 2012; Roberts and Allen, 2016).

4.3. Changes in sequential response patterns with age

The ventriloquist after-effect describes a trial-by-trial adaptive change in perceptual reports. In principle, this serial dependency in behavior may be driven by the sensory information received during the previous trial, or the participant's response committed on that trial, or a mixture of these (Park and Kayser, 2019; Van der Burg et al., 2018). Corroborating the sensory nature of the VAE, we have previously shown that in young participants the previous audio-visual discrepancy is a better predictor of the current spatial sound localization including the VAE bias than the previous motor response (Park and Kayser, 2019) (see also Van der Burg et al., 2018). Here we confirmed this sensory nature of the

VAE for the YA. However, for the OA we found the aftereffect is better explained by the previous motor response than the multisensory discrepancy. This result was consistently obtained in the group-level fit (summed-BIC) of both linear and Bayesian models to the behavioral data, and suggests a shift from sensory-driven to a behavior-driven influence of past experience with increasing age.

In speculating about the origin of this shift, we note that the trial-by-trial ventriloquist aftereffect has been linked to brain structures implied in memory (Park and Kayser, 2019). In general, memory is known to decline with age (Nyberg and Pudas, 2019), but interestingly, episodic memory seems to be more affected than procedural memory (Nyberg et al., 2012; Small, 2001). The active nature of the overt response in the present paradigm (cursor movement) may generally boost its maintenance over time compared to the sensory information (Cohen, 1989). In the OA, the reduced sensory precision of the auditory representations may also have contributed to a prevalence of the sensory memory between trials. Hence, the shift from a sensory information-based adaptive bias to a motor-based bias with age may be a multi-faceted effect arising from both a reduced episodic memory and a reduced sensory precision with age.

4.4. Conclusion

Aging seems to have limited effects on the strength of two typically observed multisensory sensory biases in spatial perception. The mechanisms shaping multisensory integration within a trial were comparable between young and older participants, including the tendency to combine evidence across two senses. In contrast, the mechanisms shaping the multisensory-aftereffect differed, suggesting a transition from a sensory- to a behavior-driven influence of past experience on subsequent choices with age, possibly related to the reduced sensory precision or memory capacity in the elderly.

ACKNOWLEDGEMENTS

This work was supported by the European Research Council (to C.K. ERC-2014-CoG; grant No 646657).

DISCLOSURE

Participants gave informed consent prior to the testing, and were compensated in cash for their participation. The study was conducted in accordance with the Declaration of Helsinki and was approved by the ethics committee of Bielefeld University. The authors declare no competing financial interests.

REFERENCES

Acerbi, L., Ma, W.J., 2017. Practical Bayesian Optimization for Model Fitting with Bayesian Adaptive Direct Search, in: Proceedings of the 31st International Conference on Neural Information Processing Systems, NIPS'17. Curran Associates Inc., Red Hook, NY, USA, pp. 1834–1844.

Angelaki, D.E., Gu, Y., DeAngelis, G.C., 2009. Multisensory integration: psychophysics, neurophysiology, and computation. Curr. Opin. Neurobiol. 19, 452–458. https://doi.org/10.1016/j.conb.2009.06.008

Baum, S.H., Stevenson, R.A., 2017. Shifts in Audiovisual Processing in Healthy Aging. Curr. Behav. Neurosci. Rep. 4, 198–208. https://doi.org/10.1007/s40473-017-0124-7

Bedard, G., Barnett-Cowan, M., 2016. Impaired timing of audiovisual events in the elderly. Exp. Brain Res. 234, 331–340. https://doi.org/10.1007/s00221-015-4466-7

Billino, J., Drewing, K., 2018. Age Effects on Visuo-Haptic Length Discrimination: Evidence for Optimal Integration of Senses in Senior Adults. Multisensory Res. 31, 273–300. https://doi.org/10.1163/22134808-00002601

Buch, E.R., 2003. Visuomotor Adaptation in Normal Aging. Learn. Mem. 10, 55–63. https://doi.org/10.1101/lm.50303

Campos, J.L., El-Khechen Richandi, G., Taati, B., Keshavarz, B., 2018. The Rubber Hand Illusion in Healthy Younger and Older Adults. Multisensory Res. 31, 537–555. https://doi.org/10.1163/22134808-00002614

Cao, Y., Summerfield, C., Park, H., Giordano, B.L., Kayser, C., 2019. Causal Inference in the Multisensory Brain. Neuron 102, 1076-1087.e8. https://doi.org/10.1016/j.neuron.2019.03.043

Chan, Y.M., Pianta, M.J., McKendrick, A.M., 2014a. Older age results in difficulties separating auditory and visual signals in time. J. Vis. 14, 13–13. https://doi.org/10.1167/14.11.13

Chan, Y.M., Pianta, M.J., McKendrick, A.M., 2014b. Reduced audiovisual recalibration in the elderly. Front. Aging Neurosci. 6. https://doi.org/10.3389/fnagi.2014.00226

Cohen, R.L., 1989. Memory for action events: The power of enactment. Educ. Psychol. Rev. 1, 57–80. https://doi.org/10.1007/BF01326550

Cressman, E.K., Salomonczyk, D., Henriques, D.Y.P., 2010. Visuomotor adaptation and proprioceptive recalibration in older adults. Exp. Brain Res. 205, 533–544. https://doi.org/10.1007/s00221-010-2392-2

DeLoss, D.J., Pierce, R.S., Andersen, G.J., 2013. Multisensory integration, aging, and the sound-induced flash illusion. Psychol. Aging 28, 802–812. https://doi.org/10.1037/a0033289

Diaconescu, A.O., Hasher, L., McIntosh, A.R., 2013. Visual dominance and multisensory integration changes with age. NeuroImage 65, 152–166. https://doi.org/10.1016/j.neuroimage.2012.09.057

Diederich, A., Colonius, H., Schomburg, A., 2008. Assessing age-related multisensory enhancement with the time-window-of-integration model. Neuropsychologia 46, 2556–2562. https://doi.org/10.1016/j.neuropsychologia.2008.03.026

Dobreva, M.S., O'Neill, W.E., Paige, G.D., 2012. Influence of age, spatial memory, and ocular fixation on localization of auditory, visual, and bimodal targets by human subjects. Exp. Brain Res. 223, 441–455. https://doi.org/10.1007/s00221-012-3270-x

Dobreva, M.S., O'Neill, W.E., Paige, G.D., 2011. Influence of aging on human sound localization. J. Neurophysiol. 105, 2471–2486. https://doi.org/10.1152/jn.00951.2010

Dully, J., McGovern, D.P., O'Connell, R.G., 2018. The impact of natural aging on computational and neural indices of perceptual decision making: A review. Behav. Brain Res. 355, 48–55. https://doi.org/10.1016/j.bbr.2018.02.001

Ernst, M.O., Banks, M.S., 2002. Humans integrate visual and haptic information in a statistically optimal fashion. Nature 415, 429–433. https://doi.org/10.1038/415429a

Falkenstein, M., Yordanova, J., Kolev, V., 2006. Effects of aging on slowing of motor-response generation. Int. J. Psychophysiol. 59, 22–29. https://doi.org/10.1016/j.ijpsycho.2005.08.004

Freiherr, J., Lundström, J.N., Habel, U., Reetz, K., 2013. Multisensory integration mechanisms during aging. Front. Hum. Neurosci. 7. https://doi.org/10.3389/fnhum.2013.00863

Hay-McCutcheon, M.J., Pisoni, D.B., Hunt, K.K., 2009. Audiovisual asynchrony detection and speech perception in hearing-impaired listeners with cochlear implants: A preliminary analysis. Int. J. Audiol. 48, 321–333. https://doi.org/10.1080/14992020802644871

Henry, M.J., Herrmann, B., Kunke, D., Obleser, J., 2017. Aging affects the balance of neural entrainment and top-down neural modulation in the listening brain. Nat. Commun. 8, 15801. https://doi.org/10.1038/ncomms15801

Henschke, J.U., Ohl, F.W., Budinger, E., 2018. Crossmodal Connections of Primary Sensory Cortices Largely Vanish During Normal Aging. Front. Aging Neurosci. 10, 52. https://doi.org/10.3389/fnagi.2018.00052

Jones, S.A., Beierholm, U., Meijer, D., Noppeney, U., 2019. Older adults sacrifice response speed to preserve multisensory integration performance. Neurobiol. Aging 84, 148–157. https://doi.org/10.1016/j.neurobiolaging.2019.08.017

Koen, J.D., Rugg, M.D., 2019. Neural Dedifferentiation in the Aging Brain. Trends Cogn. Sci. 23, 547–559. https://doi.org/10.1016/j.tics.2019.04.012

Körding, K.P., Beierholm, U., Ma, W.J., Quartz, S., Tenenbaum, J.B., Shams, L., 2007. Causal Inference in Multisensory Perception. PLoS ONE 2, e943. https://doi.org/10.1371/journal.pone.0000943

Laurienti, P.J., Burdette, J.H., Maldjian, J.A., Wallace, M.T., 2006. Enhanced multisensory integration in older adults. Neurobiol. Aging 27, 1155–1163. https://doi.org/10.1016/j.neurobiolaging.2005.05.024

Lindenberger, U., Baltes, P.B., 1994. Sensory functioning and intelligence in old age: A strong connection. Psychol. Aging 9, 339–355. https://doi.org/10.1037/0882-7974.9.3.339

Mahoney, J.R., Holtzer, R., Verghese, J., 2014. Visual-Somatosensory Integration and Balance: Evidence for Psychophysical Integrative Differences in Aging. Multisensory Res. 27, 17–42. https://doi.org/10.1163/22134808-00002444

McNair, S.W., Kayser, S.J., Kayser, C., 2019. Consistent pre-stimulus influences on auditory perception across the lifespan. NeuroImage 186, 22–32. https://doi.org/10.1016/j.neuroimage.2018.10.085

Mozolic, J.L., Hugenschmidt, C.E., Peiffer, A.M., Laurienti, P.J., 2012. Multisensory Integration and Aging, in: Murray, M.M., Wallace, M.T. (Eds.), The Neural Bases of Multisensory Processes, Frontiers in Neuroscience. CRC Press/Taylor & Francis, Boca Raton (FL).

Nasreddine, Z.S., Phillips, N.A., BÃ©dirian, V., Charbonneau, S., Whitehead, V., Collin, I., Cummings, J.L., Chertkow, H., 2005. The Montreal Cognitive Assessment, MoCA: A Brief Screening Tool For Mild Cognitive Impairment: MOCA: A BRIEF SCREENING TOOL FOR MCI. J. Am. Geriatr. Soc. 53, 695–699. https://doi.org/10.1111/j.1532-5415.2005.53221.x

Noel, J.-P., De Niear, M., Van der Burg, E., Wallace, M.T., 2016. Audiovisual Simultaneity Judgment and Rapid Recalibration throughout the Lifespan. PLOS ONE 11, e0161698. https://doi.org/10.1371/journal.pone.0161698

Nunez, M.D., 2015. Individual differences in attention influence perceptual decision making. Front. Psychol. 6. https://doi.org/10.3389/fpsyg.2015.00018

Nyberg, L., Lövdén, M., Riklund, K., Lindenberger, U., Bäckman, L., 2012. Memory aging and brain maintenance. Trends Cogn. Sci. 16, 292–305. https://doi.org/10.1016/j.tics.2012.04.005

Nyberg, L., Pudas, S., 2019. Successful Memory Aging. Annu. Rev. Psychol. 70, 219–243. https://doi.org/10.1146/annurev-psych-010418-103052

Otte, R.J., Agterberg, M.J.H., Van Wanrooij, M.M., Snik, A.F.M., Van Opstal, A.J., 2013. Age-related Hearing Loss and Ear Morphology Affect Vertical but not Horizontal Sound-Localization Performance. J. Assoc. Res. Otolaryngol. 14, 261–273. https://doi.org/10.1007/s10162-012-0367-7

Palminteri, S., Wyart, V., Koechlin, E., 2017. The Importance of Falsification in Computational Cognitive Modeling. Trends Cogn. Sci. 21, 425–433. https://doi.org/10.1016/j.tics.2017.03.011

Park, H., Kayser, C., 2019. Shared neural underpinnings of multisensory integration and trial-by-trial perceptual recalibration in humans. eLife 8, e47001. https://doi.org/10.7554/eLife.47001

Rigoux, L., Stephan, K.E., Friston, K.J., Daunizeau, J., 2014. Bayesian model selection for group studies — Revisited. NeuroImage 84, 971–985. https://doi.org/10.1016/j.neuroimage.2013.08.065

Roberts, K.L., Allen, H.A., 2016. Perception and Cognition in the Ageing Brain: A Brief Review of the Short- and Long-Term Links between Perceptual and Cognitive Decline. Front. Aging Neurosci. 8. https://doi.org/10.3389/fnagi.2016.00039

Rohe, T., Ehlis, A.-C., Noppeney, U., 2019. The neural dynamics of hierarchical Bayesian causal inference in multisensory perception. Nat. Commun. 10, 1907. https://doi.org/10.1038/s41467-019-09664-2

Rohe, T., Noppeney, U., 2015a. Sensory reliability shapes perceptual inference via two mechanisms. J. Vis. 15, 22. https://doi.org/10.1167/15.5.22

Rohe, T., Noppeney, U., 2015b. Cortical Hierarchies Perform Bayesian Causal Inference in Multisensory Perception. PLOS Biol. 13, e1002073. https://doi.org/10.1371/journal.pbio.1002073

Salthouse, T.A., 2019. Trajectories of normal cognitive aging. Psychol. Aging 34, 17–24. https://doi.org/10.1037/pag0000288

Salthouse, T.A., 2010. Influence of age on practice effects in longitudinal neurocognitive change. Neuropsychology 24, 563–572. https://doi.org/10.1037/a0019026

Salthouse, T.A., 1996. The processing-speed theory of adult age differences in cognition. Psychol. Rev. 103, 403–428. https://doi.org/10.1037/0033-295X.103.3.403

Sekiyama, K., Soshi, T., Sakamoto, S., 2014. Enhanced audiovisual integration with aging in speech perception: a heightened McGurk effect in older adults. Front. Psychol. 5. https://doi.org/10.3389/fpsyg.2014.00323

Setti, A., Burke, K.E., Kenny, R., Newell, F.N., 2013. Susceptibility to a multisensory speech illusion in older persons is driven by perceptual processes. Front. Psychol. 4. https://doi.org/10.3389/fpsyg.2013.00575

Setti, A., Finnigan, S., Sobolewski, R., McLaren, L., Robertson, I.H., Reilly, R.B., Anne Kenny, R., Newell, F.N., 2011. Audiovisual temporal discrimination is less efficient with aging: an event-related potential study. NeuroReport 22, 554–558. https://doi.org/10.1097/WNR.0b013e328348c731

Simmons, J.P., Nelson, L.D., Simonsohn, U., 2011. False-Positive Psychology: Undisclosed Flexibility in Data Collection and Analysis Allows Presenting Anything as Significant. Psychol. Sci. 22, 1359–1366. https://doi.org/10.1177/0956797611417632

Small, S.A., 2001. Age-Related Memory Decline: Current Concepts and Future Directions. Arch. Neurol. 58. https://doi.org/10.1001/archneur.58.3.360

Smith, G.A., Brewer, N., 1995. Slowness and age: Speed-accuracy mechanisms. Psychol. Aging 10, 238–247. https://doi.org/10.1037/0882-7974.10.2.238

Sokal, R.R., Rohlf, F.J., 1981. Biometry: the principles and practice of statistics in biological research, 2d ed. ed. W. H. Freeman, San Francisco.

Starns, J.J., Ratcliff, R., 2010. The effects of aging on the speed–accuracy compromise: Boundary optimality in the diffusion model. Psychol. Aging 25, 377–390. https://doi.org/10.1037/a0018022

Trelle, A.N., Henson, R.N., Simons, J.S., 2019. Neural evidence for age-related differences in representational quality and strategic retrieval processes. Neurobiol. Aging 84, 50–60. https://doi.org/10.1016/j.neurobiolaging.2019.07.012

Tye-Murray, N., Spehar, B., Myerson, J., Hale, S., Sommers, M., 2016. Lipreading and audiovisual speech recognition across the adult lifespan: Implications for audiovisual integration. Psychol. Aging 31, 380–389. https://doi.org/10.1037/pag0000094

Van der Burg, E., Alais, D., Cass, J., 2018. Rapid recalibration to audiovisual asynchrony follows the physical—not the perceived—temporal order. Atten. Percept. Psychophys. 80, 2060–2068. https://doi.org/10.3758/s13414-018-1540-9

Vercillo, T., Carrasco, C., Jiang, F., 2017. Age-Related Changes in Sensorimotor Temporal Binding. Front. Hum. Neurosci. 11, 500. https://doi.org/10.3389/fnhum.2017.00500

Wozny, D.R., Beierholm, U.R., Shams, L., 2010. Probability Matching as a Computational Strategy Used in Perception. PLoS Comput. Biol. 6, e1000871. https://doi.org/10.1371/journal.pcbi.1000871

Wozny, D. R., Shams, L., 2011. Recalibration of Auditory Space following Milliseconds of Cross-Modal Discrepancy. J. Neurosci. 31, 4607–4612. https://doi.org/10.1523/JNEUROSCI.6079-10.2011

Wozny, David R., Shams, L., 2011. Computational Characterization of Visually Induced Auditory Spatial Adaptation. Front. Integr. Neurosci. 5. https://doi.org/10.3389/fnint.2011.00075

Zanto, T.P., Gazzaley, A., 2014. Attention and Ageing. Oxford University Press. https://doi.org/10.1093/oxfordhb/9780199675111.013.020

Zou, Z., Chau, B.K.H., Ting, K.-H., Chan, C.C.H., 2017. Aging Effect on Audiovisual Integrative Processing in Spatial Discrimination Task. Front. Aging Neurosci. 9, 374. https://doi.org/10.3389/fnagi.2017.00374